ISSN 1063-7710, Acoustical Physics, 2016, Vol. 62, No. 5, pp. 545–553. © Pleiades Publishing, Ltd., 2016.
Original Russian Text © V.S. Gostev, A.V. Mikryukov, O.E. Popov, 2016, published in Akusticheskii Zhurnal, 2016, Vol. 62, No. 5, pp. 540–549.

OCEAN ACOUSTICS. HYDROACOUSTICS

Features of Sound Propagation in the Ocean with Fine-Structure Inhomogeneities

V. S. Gostev, A. V. Mikryukov, and O. E. Popov

JSC Concern Morinformsystema AGAT

Andreev Acoustics Institute, ul. Shvernika 4, Moscow, 117036 Russia

e-mail: olegp@mail.ru

Received December 16, 2015

Abstract—We analyze the results of an experiment using an explosive sound source in the tropical part of the Indian Ocean. We consider the time structure of sound signals in geometric shadow zones to a distance of 270 km and the scheme of how the sound field in the shadow zone is formed by rays reflected from horizontally extended fine-structured sound velocity layers. From the results of calculation using a wave program that realizes the method of psuedodifferential parabolic equations, we analyze the influence of signal scattering by fine-structure sound velocity inhomogeneities on the sound field distribution in a waveguide. We show that the field formed by spots of light in each of the shadow zones is generated by a regular field and propagates in parallel to it, taking energy from the regular zone in the near field and in each subsequent convergence zone. This mechanism causes an additional decrease in the field in illuminated zones, which can be interpreted as additional attenuation of the regular sound field.

Keywords: ocean acoustics, shadow zone, fine-structure thermohaline inhomogeneities of the ocean, method of pseudodifferential parabolic equations

DOI: 10.1134/S106377101605002X

Studies of fine-structured thermohaline inhomogeneities of an oceanic medium have led to the understanding that an oceanic medium is strongly stratified. In contrast to earlier notions on sound scattering in the ocean by small-scale locally isotropic sound velocity inhomogeneities, a model of an oceanic medium was proposed that had sharply anisotropic, horizontally extended, fine-structured inhomogeneities [1].

When sound is scattered by such inhomogeneities, the maximum of the scattered energy appears not only in the direction of sound wave propagation, but also in the direction of the mirror reflection angle for horizontally extended fine-structured inhomogeneities.

As a result, sound penetrates into domains forbidden by geometric acoustics, in particular, into acoustic shadow zones. A sound field in a shadow zone is thus created owing to signals not only reflected from the bottom, but also mirror-reflected from layers with a sharpened vertical sound velocity gradient (Epstein layers [2]) or resonantly scattered by fine-structured diffraction gratings of the corresponding period, like Wolf–Bragg diffraction. Analysis of the propagation paths of sound mirror-reflected from a fine structure has shown that the field at a given point of the shadow zone is mainly formed by rays reflected only in individual spatial domains insonified by the primary wave when there are caustics from the primary field [3]. These domains, being domains of substantial reflection, form in the shadow zone a multiray structure of the reflected sound signal observed in experiment. In such insonified shadow zones, the scattered component of the sound field can be considered, on the one hand, as a reverberation disturbance, and on the other, as a source of additional information when solving hydroacoustic problems.

Earlier signals penetrating the first shadow zone were studied in [4]. Work [5] considered the scheme by which the field was formed in the shadow zone by rays mirror-reflected from horizontally extended fine-structured layers. It was shown that for given emission and reception points, it is possible to select an occurrence depth of a layered inhomogeneity such that rays mirror-reflected from it form caustics at the reception point. A narrow beam mirror-reflected from such an inhomogeneity can make the main contribution to the field at a reception point located in a shadow zone—we call it a "flare." Using these concepts, the authors of [6] analyzed the experimental angular and time structure of a sound field in the first shadow zone. In addition, in [4], it was concluded that it is possible to insonify not only the first, but also farther shadow zones, since in each convergence zone sound energy is transferred from a regular field to the field of flares insonifying subsequent shadow zones.

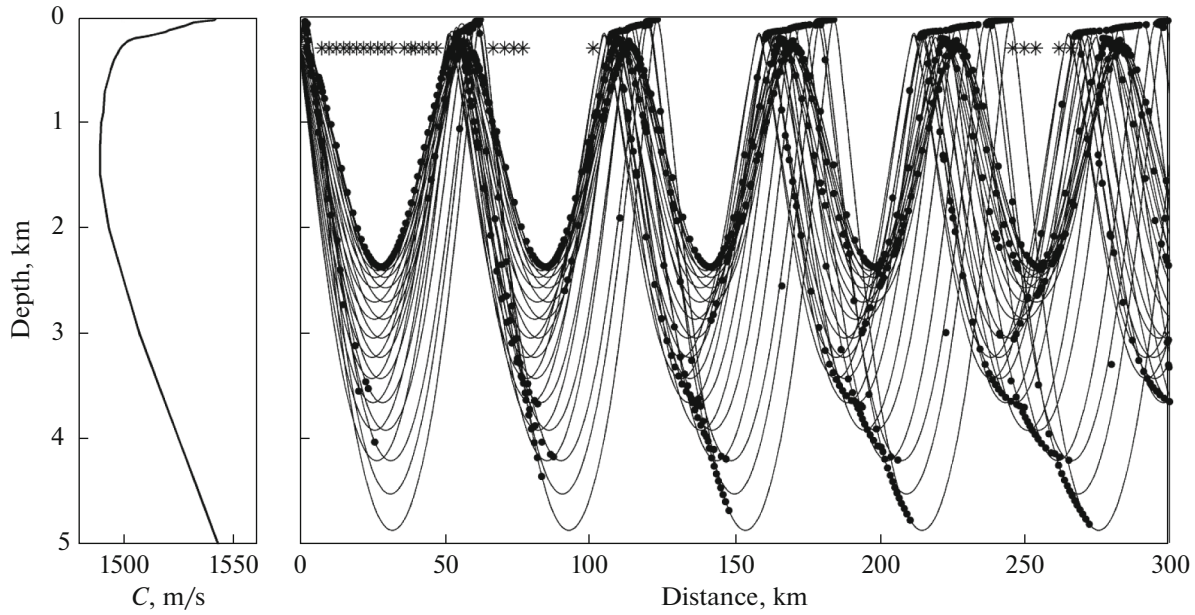

Fig. 1. Sound velocity profile and ray pattern of sound field. * marks explosion points. Black dots are places with caustics.

This paper presents the results of experimental investigations on the penetration of signals from an explosive sound source into deep-ocean shadow zones, from the first to the fifth inclusive. The experiment was conducted in the tropical zone of the Indian Ocean on a track extending 300 km at a depth of 5 km. Charges weighing 2.5 kg were detonated at a depth of 300 m from a vessel traveling at full speed. Signals were received by a single undirected hydrophone at a depth of 300 m in the frequency band of 20–2500 Hz and by 20 undirected hydrophones of a vertical chain with the center at a depth of 300 m, spaced 2 m from each other, in the frequency band of 500–3500 Hz. Signal reception by the chain of hydrophones made it possible to estimate the angle of arrival of individual signals by their time delays, thereby increasing the reliability of their identification.

Figure 1 shows the sound velocity profile and ray pattern of the sound field along the experimental track. Calculation was performed for purely water rays to determine the arrangement of illuminated and shadow zones. Asterisks at the 300 m depth level denote the distances at which explosion signals were detected in the shadow zones. The ray calculation of the sound field shown in Fig. 1 demonstrates the starkly pronounced zonality and the presence of caustics, which is characteristic of tropical areas of the World Ocean, which differ in the spatial stability of the vertical sound velocity profile.

Figure 2 shows the explosive signals detected in the first, second, and fifth shadow zones in the frequency range of 500–3500 Hz. For all signals, the scale of the horizontal and vertical axes is constant.

In Fig. 2, the first to arrive are leakage signals, which initially propagate in the near-surface channel. At the beginning of the shadow zone (246 km), water signals arrive together with leakage signals. Following them are the above-mentioned flares, superposed with respect to short signals. The arrivals of the fastest flare signals in Fig. 2 are brought to zero on the time scale. Then follow bottom reflections, shown in the first shadow zone with amplitude restrictions. This order of signal arrival is retained for all shadow zones. The solid lines show the calculated lead times of leakage signals; thick lines show the delay of bottom reflections with respect to the calculated propagation times of the fastest flares; the dashed curve shows the calculated duration of flares (with respect to zero).

It can be seen that the experimentally recorded level of flare signals is approximately the same in all shadow zones. Meanwhile, the level of bottom reflections is substantially decreased, and in the fifth shadow zone, it barely manifests itself on the background of natural noise. One can see in Fig. 2 that when the second (102 km) and fifth (266 km) convergence zones are approached, a direct water signal appears, which flares overlap, weakening the prereverberation of the direct signal [4]. The experimental results in the fifth shadow zone are considered in detail in [7].

Leakages and bottom reflections are quite simply identified both by shape and by comparison with ray calculations of their propagation times [4]. The shape of a flare represents some reverberation signal and sharply differs in shape both from leakages, which have a simply structure and consist of a shock wave and a pulsation, and from bottom reflection signals

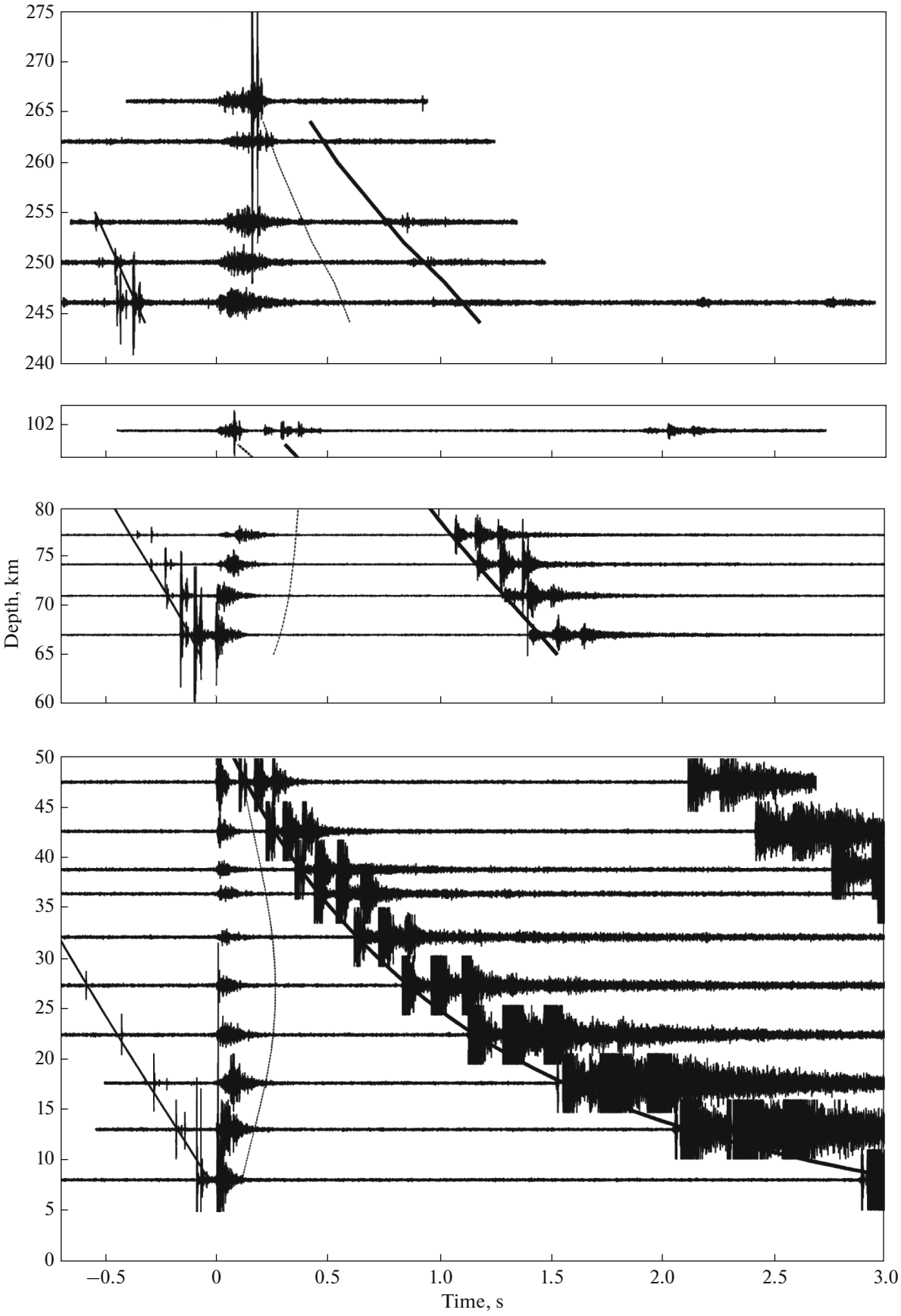

Fig. 2. Explosion signals detected in first, second, and fifth shadow zones in frequency range of 500–3500 Hz.

containing three or four discrete arrivals depending on the ratio of the emission and reception depths.

To calculate and analyze the time structure of flares at a given reception point, it is necessary to consider all possible variants of their formation by signals mirror-reflected from layered inhomogeneities. In the first shadow zone, flares are formed by sound mirror-reflected upward from layered inhomogeneities and arriving at the reception point from above and below. In all subsequent shadow zones, flares are formed by sound reflected upward from layered inhomogeneities and arriving at a given point from above and below, as well as by sound reflected downward and also arriving at a given point from above and below.

The subsequent analysis uses the following principle of reduced notation of families of rays forming flares: the first letter represents rays departing downward (D) or upward (U) from the source; the second letter, rays reflected downward (D) or upward (U) from inhomogeneities; and the third letter, rays arriving at the reception point from below (D) or above (U).

To find the trajectories of rays reflected from fine-structured inhomogeneities and arriving at the reception point, the following algorithm was applied. Let us consider the simplest case of equality of the emission and reception depth levels. At the first stage, for each ray departing from the source, the complete cycle of ray D and two semicycles, upper D_s and lower D_b, are calculated:

$$D = D_s + D_b.$$

For the given distance between the source and receiver r and calculated D_s and D_b, the distance R is calculated at which the ray incident on the reception point is reflected from a fine-structured inhomogeneity (R_u for rays arriving to the receiver from above and R_D, from below). Then, the trajectory of this ray is calculated to distance R and the depth of the ray z is determined at this distance. For ray families UUU, DUD, and the reception point located in the first shadow zone at a depth equal that of the source, distance R for all rays will be equal to $r/2$ (the ray trajectories are symmetric with respect to the vertical passing through point R). By calculating the ray trajectory to point R, it is possible to obtain the dependence of the depths of reflection points on the angle of arrival of a ray from the source, as well as the propagation times. For ray families UUD and DUU, in the first shadow zone, distance R is determined from the formulas $R_D = (r + D_s)/2$ and $R_U = (r - D_s)/2$, respectively. Calculating the ray trajectory up to this distance, we obtain the dependence of the reflection depths and propagation times on the angle of arrival for the given families. In the general case, distance R at which a ray incident on a given reception point in the shadow zone is mirror-reflected from a fine-structured inhomogeneity can be calculated for all above-mentioned ray families by the following formulas:

$$\begin{aligned}
&\text{UUU} \quad R_U = LD + dr/2,\\
&\text{UUD} \quad R_D = R_U + D_s/2,\\
&\text{DUU} \quad R_U = LD + (dr - D_s)/2,\\
&\text{DUD} \quad R_D = R_U + D_s/2,\\
&\text{UDU} \quad R_U = LD - (D - dr)/2,\\
&\text{UDD} \quad R_D = R_U + D_s/2,\\
&\text{DDU} \quad R_U = (L-1)D + (D_s + dr)/2, \quad L \neq 0,\\
&\text{DDD} \quad R_D = R_U + D_s/2,
\end{aligned} \tag{1}$$

where $dr = r - ND$ is the difference between the distance of the location of the reception point is located and the distance for the number of complete ray cycles (N is the number of complete cycles); $L = 0, 1, 2, \ldots$ is the number of the convergence zone in which a ray undergoes mirror reflection from layered structures and $L < N$ ($L = 0$ is the near field). The formulas are valid for a deep shadow zone when the number of complete cycles is the same for all rays.

For an emission depth not equal to the reception depth, at the first stage of ray calculation it is necessary to determine another parameter: the difference in distances at which the ray intersects the depth levels of the emitter and receiver.

Let us consider the flare formation pattern in the first shadow zone at a distance of 10 km from the source (emission and reception depths of 300 m). Figure 3 shows the ray families DDU and UUD.

In addition to these two ray families in the first shadow zone, there are two more: UUU and DUD. These families will be symmetric, and all reflection points will lie on the vertical, located 5 km from the source.

Figure 4 shows the depths of mirror-reflection points for rays in the first shadow zone incident on a given point at a distance of 10 km from all four of the above-mentioned families as a function of the angle of departure from the source and the sound propagation time of the corresponding rays. The reflection depth curves have local extrema, which correspond to the local extrema of the sound propagation times for the considered ray trajectories. These domains of local depth extrema are domains of substantial reflection for the given reception point from which reflected sound will arrive at the reception point as a bundle of rays in phase with each other and create a flare in the shadow zone. The maximum duration of the total flare signal will be determined by the time scatter of local propagation time extrema for all ray families.

In [5] it was shown that a receiver located in a shadow zone receives sound propagating over individual ray families mirror-reflected from layered structures and forming caustics at the reception point. This is illustrated in Fig. 5, which visually demonstrates the

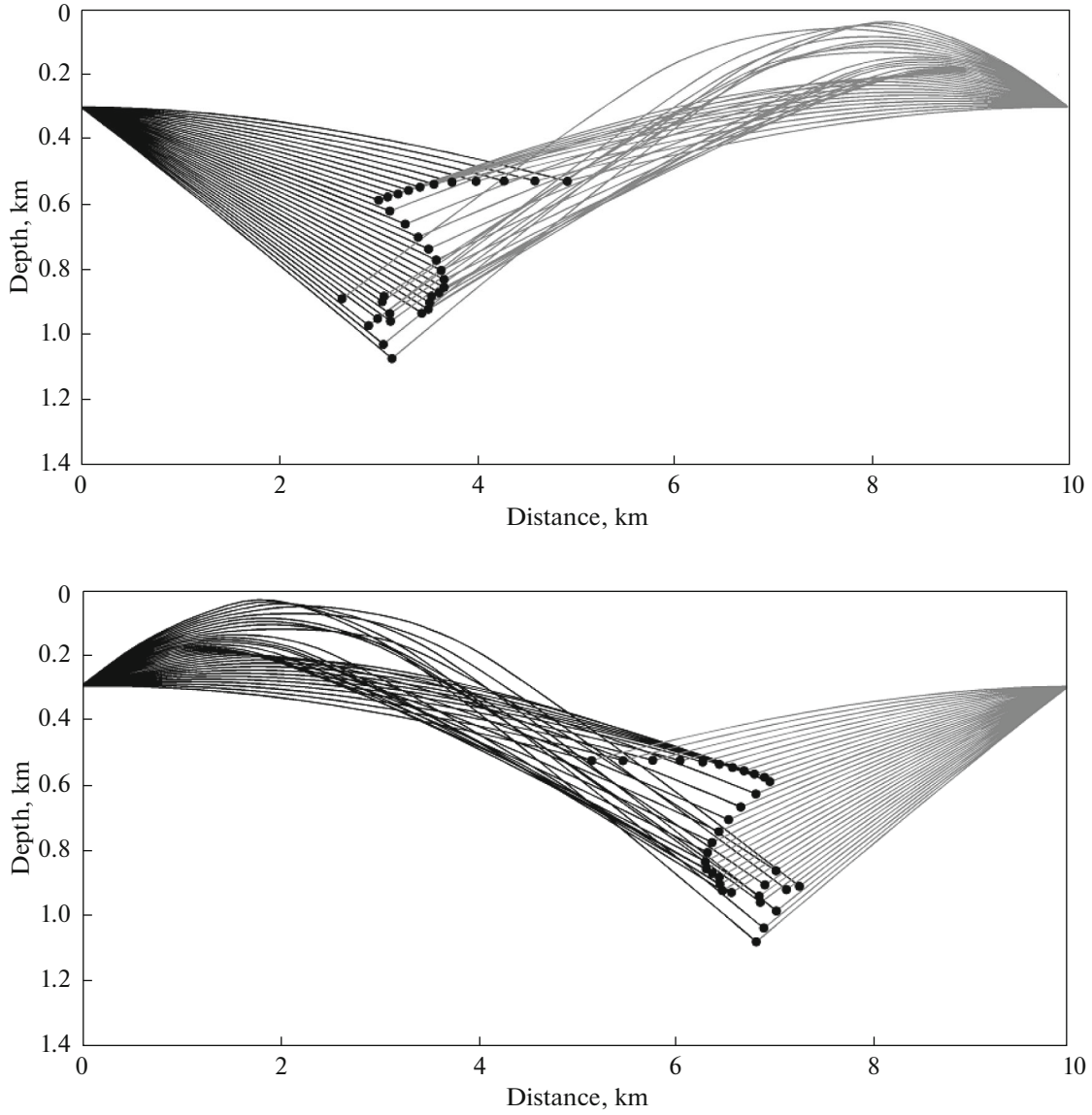

Fig. 3. Rays reflected from layered inhomogeneities and incident on given reception point at distance of 10 km (depth 300 m): upward, DUU; downward, UUD.

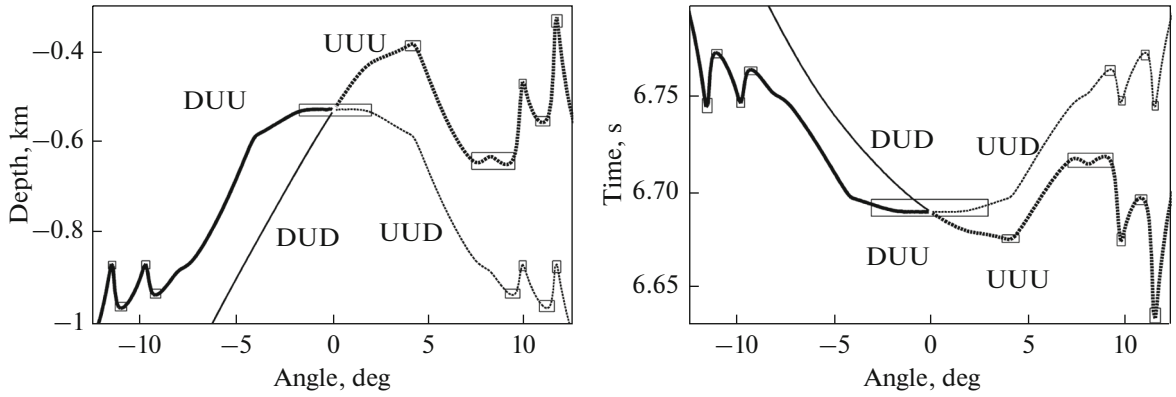

Fig. 4. Dependence of depths of points of mirror-reflection of rays arriving at reception point (left) and dependence of sound propagation times for rays arriving at reception point (right) on angle of departure from source. Rectangles highlight local extrema.

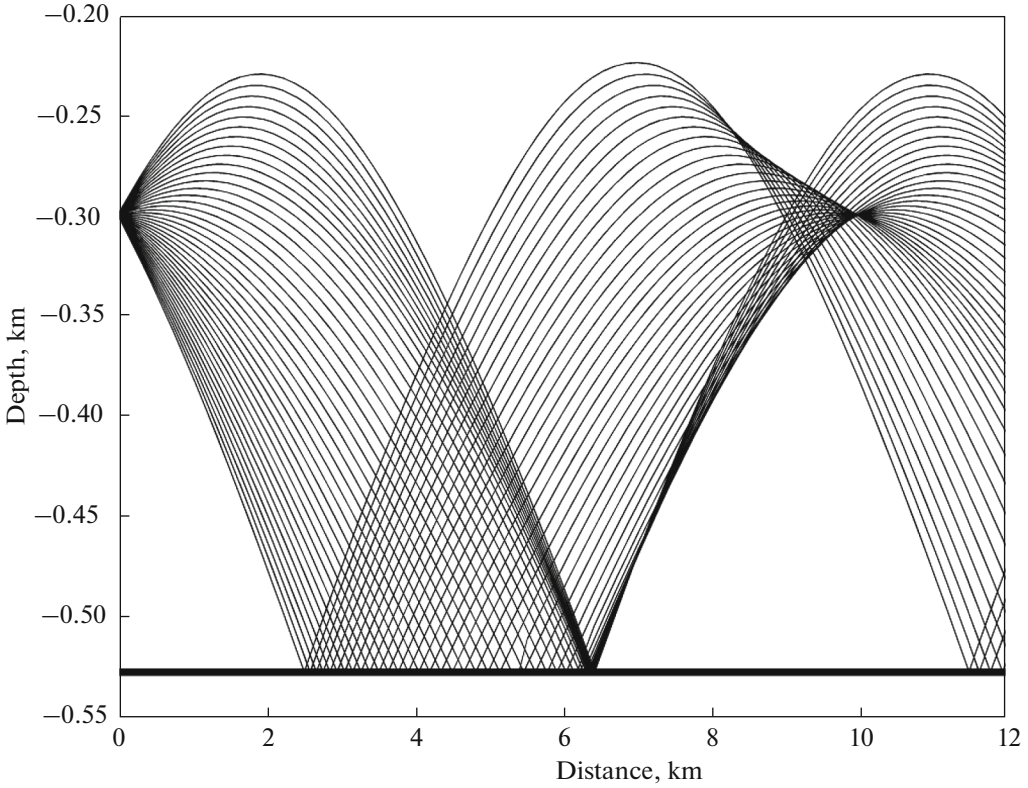

Fig. 5. Rays with angles of departure from source from −1° to +1° reflected from extended inhomogeneity at depth of 528 m.

physical sense of local extrema in Fig. 4. This figure shows rays reflected from an extended inhomogeneity at a depth of 528 m (the most significant extremum for an angle of departure of −1° to +1° (families DUU and UUD, Fig. 3). Clearly, a receiver at a depth of 300 m and a distance of 10 km is located at the intersection of caustics generated by bundles of rays with small angles of departure, which are focused at this point and correspond to the arrivals of flares from above and below.

In the second shadow zone, along with the flares formed by rays from the near field during reflection upward from layered inhomogeneities (four families), flares appear, formed by the system of rays from the first convergence zone (eight families). From these, for ray families are reflected upward from layered inhomogeneities (DUU, DUD, UUU, and UUD) and four downward. In the flat-layered model of the medium used by us, the propagation time of flares, as well as their formation depth from the near field and from the first convergence zone in the same family, will be the same. There intensities will also be equal. Thus, the flares of each family in the second shadow zone will consist of flares formed in the near field and flares from the first convergence zone. Such a scheme by which the flare field forms is applicable for all shadow zones.

Based on the example of formation of the scattered field in the second shadow zone, it is possible to conclude that, starting from the second shadow zone, the number of ray families participating in the formation of the flare field in the given zone will increase by eight each time.

The mean energy insonifying the subsequent shadow zone from the convergence zone in each of the ray families will be E_{UUU}, E_{UUD}, etc. Then, the total flare energy insonifying the Mth shadow zone will be

$$\begin{aligned} E &= M(E_{UUU} + E_{UUD} + E_{DUU} + E_{DUD}) \\ &+ (M-1)(E_{UDU} + E_{UDD} + E_{DDU} + E_{DDD}) \\ &= ME_U + (M-1)E_D, \end{aligned}$$

i.e., the total number of ray families, each of which can yield several flares forming the signal, will be equal to

$$N = 4 + 8(M-1), \qquad (2)$$

where $M = 1, 2, 3, \ldots$ is the number of the shadow zone.

Thus, it is possible to calculate all the ray characteristics of flares: the propagation times, the angles of arrival, and the location of the domains of substantial reflection in the space. The considered kinematic ray model of flare formation does not give the energy characteristics of the flare field. In order for the ray program to calculate the flare intensity, it it necessary

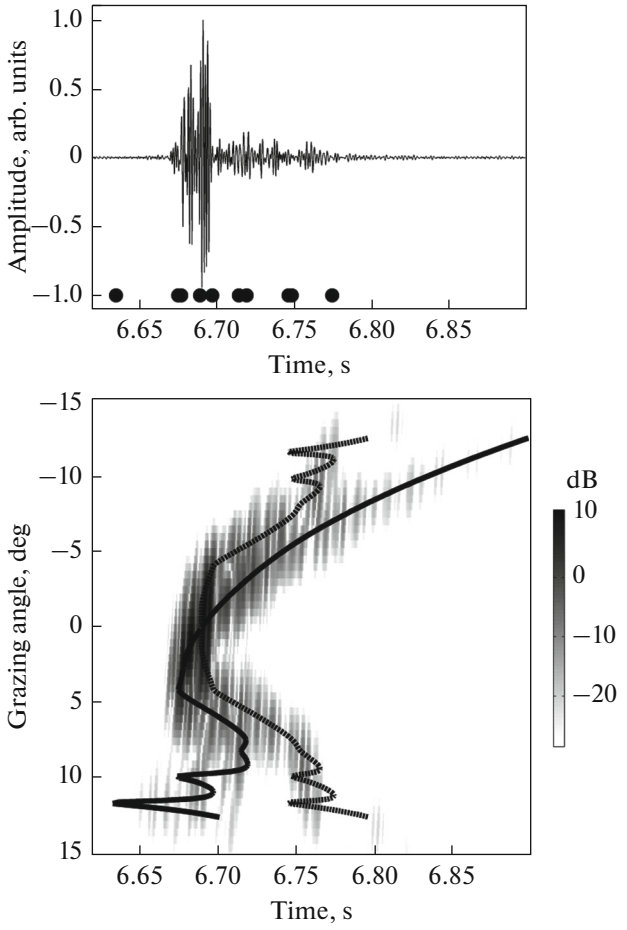

Fig. 6. Top: flare signal calculated by PDPE wave program in first shadow zone at distance of 10 km for profile with fine-structured addition. Points show flare propagation times calculated by ray program. Bottom: halftone image of time dependence of angle structure of sound field. Lines show dependence of sound propagation times for rays arriving at reception point on angle of departure from source.

to know the spatial characteristics of fine-structured inhomogeneities in the domain of its formation, to calculate the intensity of its reflection or scattering in this domain, and to know the degree of ray focusing in the reflection domain and at the reception point.

To calculate the intensity of the flare field, K.V. Avilov's program was used [8], which implemented the psuedodifferential parabolic equation (PDPE) method. The PDPE program makes it possible to take into account the considered mechanism by which flares form as sound propagates in the ocean and to obtain the energy characteristics of both the regular and scattered field.

The top of Fig. 6 shows the results of the PDPE program's calculation of a signal in the first shadow zone at a distance of 10 km for the flat-layered model for the profile in Fig. 1 with the introduction of a fine-structured addition for a source and receiver depth of 300 m. The parameters of the fine-structured addition of the sound velocity are as follows: the spectral slope is inversely proportional to the square of the spatial wavenumber of fluctuations in inhomogeneities, a dispersion near the surface of 0.1 m/s that monotonically decreases with depth exponentially with an attenuation decrement of 1500 m [9]. The maximum signal amplitude is brought to unity. The signal in the source was given in the form of a delta function filtered in the frequency band of 300–800 Hz. Dots show the flare propagation times calculated by the ray program. During calculations for a profile without the fine-structured addition, flare signals are not observed.

The bottom of Fig. 6 shows the calculated dependence of the angle structure of the sound field on time as a halftone image. The image was obtained by simulated angle scanning in the vertical plane by an array at a height of 80 m, the center of which was at a depth of 300 m. For comparison, this figure also shows the calculated dependence of the sound propagation times for rays arriving at the reception point on the angle of departure from the source (just like in Fig. 4).

This example shows that the PDPE program takes into account the above-mentioned mechanism of flare formation and makes it possible to calculate flare signals.

Let us compare the energy characteristics of the sound field in the shadow and convergence zones for the smoothed sound velocity profile and the profile with the fine-structured addition. Figure 7 shows the calculation results in the 1/3-octave band with a central frequency of 1000 Hz of the horizontal profiles of the sound field to a distance of 300 km at a source and receiver depth of 300 m (ignoring sound attenuation).

It is possible to see the following characteristic differences. For the profile with the fine-structured addition, the field levels in the shadow zones owing to flares prove significantly higher; the difference reaches 40 dB in the first shadow zone and almost 25 dB in the second. In all five shadow zones, the level of the sound field generated by flares not only drops with increasing zone number, it also somewhat increases. This occurs also because attenuation of the scattered field in the shadow zones in accordance with the cylindrical law is compensated by the transfer of energy from the regular field to the flare field, and the number of ray families yielding flares of each subsequent zone increases by eight.

Let us approximately estimate the change in intensity of a signal generated by flares with increasing shadow zone number. We will consider that the number of flares is directly proportional to the number of ray families, the intensity of all flares at the reception point is the same, and flare signals are added energetically. The distance to the middle of the shadow zone with number M is approximately equal to $25 + 60(M - 1)$ km. Then, taking into account the increase in the number of ray families (2) and attenu-

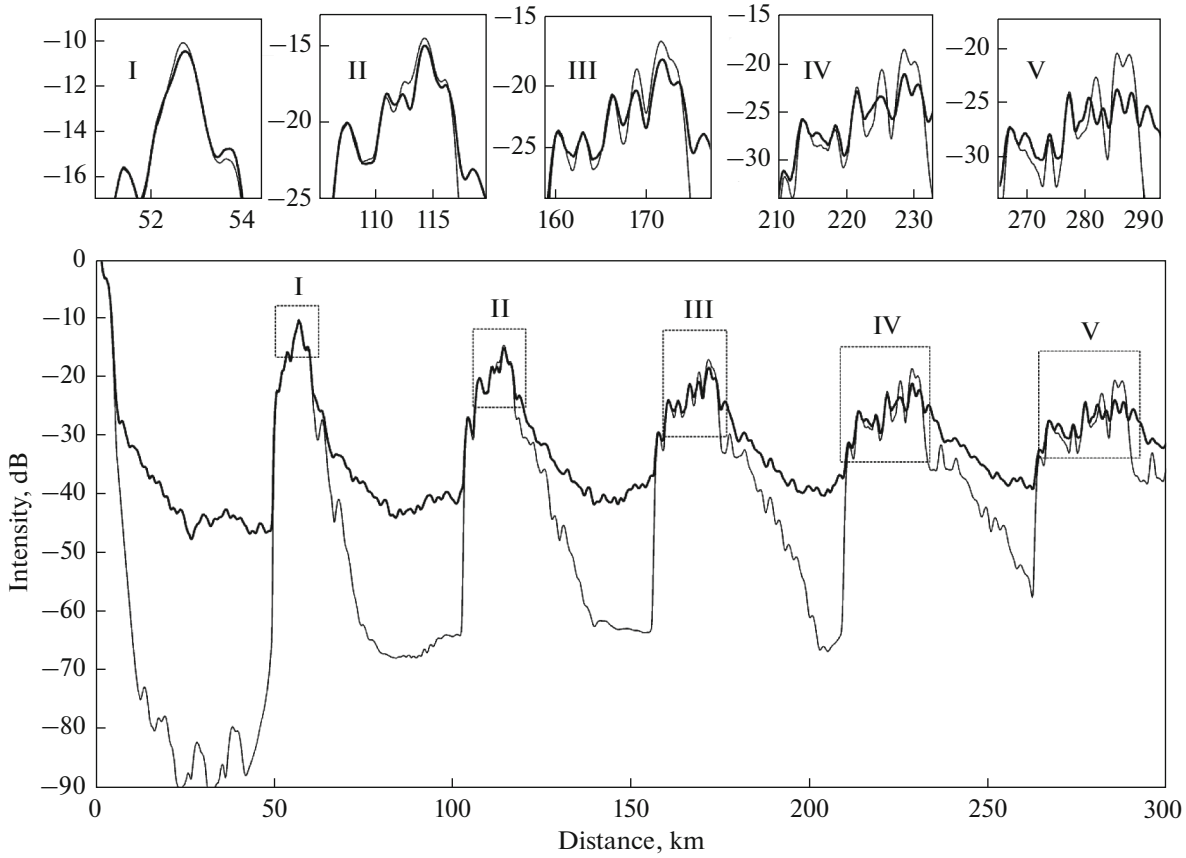

Fig. 7. Sound field calculated from smoothed sound velocity profile (thin curve) and for profile with fine-structured addition (thick curve). Insets show detailed construction of field in convergence zones (I–V).

ation of the scattered field in the shadow zones according to the cylindrical law, the intensity of the total flare signal in the shadow zone will be directly proportional to the following quantity W:

$$W = \frac{4 + 8(M-1)}{25 + 60(M-1)}. \quad (3)$$

The ratios of W calculated by (3) are equal to the ratio of intensities of the total flare signals in the $(M-1)$th and Mth shadow zones and are close to unity: for zones 1 and 2, this is 1.13; for zones 2 and 3, 1.02; for zones 3 and 4, 1.01; and for zones 4 and 5, 1.005.

In addition, it should be noted that the transfer of sound energy from the regular field to the flare field leads to a decrease in the maximum field levels in the convergence zones. As well, with increasing zone number, there is an increase in the difference in the sound field level calculated for the smoothed sound velocity profile and for the profile with the fine-structured addition.

For the first to fifth convergence zones—Fig. 7 (see insets with detailed construction of the field in the zones)—the differences in the maximum intensity values were calculated for the smoothed sound velocity profile and for the profile with the fine-structured addition: 0.33, 0.48, 1.4, 2.57, and 3.38 dB, respectively. These differences can be interpreted as additional attenuation around 0.084 dB/km at a central calculation frequency of 1000 Hz, which makes up 20% of conventional attenuation at the given frequency (on average, according to different estimates, around 0.04 dB/km).

The calculated intensity ratios in the illumination and shadow zones are close to those observed in experiment [7]. Thus, it can be considered that the proposed parameters of the fine-structured addition for calculation by K.V. Avilov's PDPE program make it possible with sufficient accuracy to predict the energy characteristics of flares observed in experiment.

In summary, we can say that the presence of a fine-structured component in the sound velocity profile results in the appearance of flares in the shadow zone—signals that are mirror-reflected from fine-structured sound velocity inhomogeneities. The considered kinematic model of sound penetration into a shadow zone makes it possible to unambiguously calculate for a given point in space the propagation time and angles of arrival of given signals and to show the localized domain of their reflection. Signals reflected

from horizontally extended layers of the fine structure of the sound velocity field illuminate not only the first, but also farther shadow zones, in particular, in the considered example, the fifth shadow zone. The presence of fine-structured inhomogeneities leads to the appearance in the sound signal of a reverberation component with a flare nature. In experiments, this can manifest itself as partial noise contamination of water signals (preverberation, reverberation) in spatial pulsations of the sound field in regions of transition from a shadow zone to a convergence zone [3], which can be explained by interference of individual flares.

The field formed by flares in each of the shadow zones is generated by the regular field and propagates in parallel to it, taking energy from the regular field in the near zone and in each subsequent convergence zone. This mechanism causes an additional increase in the field in illumination zones, which can be interpreted as additional attenuation of the regular sound field. With increasing zone number, the scattered field in the shadow zone can become dominant compared to bottom reflections. K.V. Avilov's PDPE wave program makes it possible to automatically take into account the considered mechanism of forming flares as sound propagates in the ocean and to calculate the energy characteristics of both the regular and scattered field.

By conducting detailed experimental studies of the flare field in shadow zones, important information can be obtained on the characteristics of fine-structured stratification in the ocean, the distribution of fine-structured depth inhomogeneities, and their spectral composition and time variability.

All of the above was considered using the model of a flat-layered medium in which the ray interpretation of flare field formation can be conducted quite simply. In the case of spatial variability of the sound velocity profile along the propagation track, such a visual interpretation is difficult. Nevertheless, it can be assumed that in the case of relatively weak variability of the sound velocity profile along the propagation track, both the regular field and the flare field are constructed identically with a change in the sound velocity profile as they propagate; the flare formation mechanism in principle remains the same. The experimental data obtained in the considered area of the ocean is evidence for the high stability of the sound velocity field along the propagation track (which is characteristic of tropical regions of the World Ocean) and, correspondingly, evidence for possible application of the model of a flat-layered medium in this case.

ACKNOWLEDGMENTS

The authors are grateful to K.V. Avilov for the use of his program for calculations. The work was supported by the Russian Foundation for Basic Research (project nos. 13-05-00268 and 15-52-40003).

REFERENCES

1. V. S. Gostev and R. F. Shvachko, Dokl. Akad. Nauk SSSR **282**, 1082 (1985).
2. L. M. Brekhovskikh, *Waves in Layered Media* (Nauka, Moscow, 1973) [in Russian].
3. V. S. Gostev, V. I. Neklyudov, S. D. Chuprov, L. V. Shvachko, and R. F. Shvachko, in *Acoustics of Ocean Medium* (Nauka, Moscow, 1989), pp. 88–97 [in Russian].
4. V. S. Gostev, L. N. Nosova, and R. F. Shvachko, Acoust. Phys. **44**, 162 (1998).
5. V. S. Gostev and R. F. Shvachko, *Proc. 9th School-Semin. acad. L. M. Brekhovskikh, GEOS, Moscow,* 2002*),* pp. 120–123.
6. S. V. Burenkov, V. S. Gostev, N. I. Knyazeva, S. S. Naumov, R. F. Shvachko, Acoust. Phys. **41**, 336 (1995).
7. V. S. Gostev, A. V. Mikryukov, O. E. Popov, and R. F. Shvachko, *Proc. 14th School-Semin. acad. L. M. Brekhovskikh, GEOS, Moscow,* 2013, pp. 41–44.
8. K. V. Avilov, Acoust. Phys. **41**, 1 (1995).
9. V. S. Gostev, O. E. Popov, and R. F. Shvachko, Acoust. Phys. **49**, 662 (2003).

Translated by A. Carpenter